Geoscience Frontiers 8 (2017) 541–553

HOSTED BY

Contents lists available at ScienceDirect

China University of Geosciences (Beijing)

Geoscience Frontiers

journal homepage: www.elsevier.com/locate/gsf

Research paper

Petrology, genesis and geodynamic implication of the Mesoproterozoic–Late Cretaceous Timmasamudram kimberlite cluster, Wajrakarur field, Eastern Dharwar Craton, southern India

Ashish Dongre [a], N.V. Chalapathi Rao [b,*], K.S. Viljoen [a], B. Lehmann [c]

[a] Department of Geology, University of Johannesburg, P.O. Box 524, Auckland Park, 2006, South Africa
[b] Department of Geology, Centre of Advanced Study, Banaras Hindu University, Varanasi 221005, India
[c] Mineral Resources, Technical University of Clausthal, 38678 Clausthal-Zellerfeld, Germany

ARTICLE INFO

Article history:
Received 7 March 2016
Received in revised form
1 May 2016
Accepted 9 May 2016
Available online 6 June 2016

Keywords:
Kimberlite
Orangeite
Diamond
Timmasamudram
Wajrakarur
India

ABSTRACT

New mineralogical and bulk-rock geochemical data for the recently recognised Mesoproterozoic (ca. 1100 Ma) and late Cretaceous (ca. 90 Ma) kimberlites in the Timmasamudram cluster (TKC) of the Wajrakarur kimberlite field (WKF), Eastern Dharwar Craton, southern India, are presented. On the basis of groundmass mineral chemistry (phlogopite, spinel, perovskite and clinopyroxene), bulk-rock chemistry (SiO_2, K_2O, low TiO_2, Ba/Nb and La/Sm), and perovskite Nd isotopic compositions, the TK-1 (macrocrystic variety) and TK-4 (Macrocrystic variety) kimberlites in this cluster are here classified as orangeites (i.e. Group II kimberlites), with geochemical characteristics that are very similar to orangeites previously described from the Bastar Craton in central India, as well as the Kaapvaal Craton in South Africa. The remaining kimberlites (e.g., TK-2, TK-3 and the TK-1 microcrystic variant), are more similar to other 1100 Ma, Group I-type kimberlites of the Eastern Dharwar Craton, as well as the typical Group I kimberlites of the Kaapvaal Craton. Through the application of geochemical modelling, based on published carbonated peridotite/melt trace element partition coefficients, we show that the generation of the TKC kimberlites and the orangeites results from low degrees of partial melting of a metasomatised, carbonated peridotite.

Depleted mantle (T_{DM}) Nd perovskite model ages of the 1100 Ma Timmasamudram kimberlites show that the metasomatic enrichment of their source regions are broadly similar to that of the Mesoproterozoic kimberlites of the EDC. The younger, late Cretaceous (ca. 90 Ma) TK-1 (macrocrystic variant) and TK-4 kimberlites, as well as the orangeites from the Bastar Craton, share similar Nd model ages of 1100 Ma, consistent with a similarity in the timing of source enrichment during the amalgamation of Rodinia supercontinent. The presence of late Cretaceous diamondiferous orangeite activity, presumably related to the location of the Marion hotspot in southern India at the time, suggests that thick lithosphere was preserved, at least locally, up to the late Cretaceous, and was not entirely destroyed during the breakup of Gondwana, as inferred by some recent geophysical models.

1. Introduction

Wagner (1914) recognized two main sub-groups of diamond-bearing rocks in South Africa, and termed them 'basaltic' and 'micaceous' kimberlites. Smith (1983) subsequently recognized that these sub-groups display distinct isotopic characteristics, and proposed the terms 'Group I' for the 'basaltic' kimberlites (less radiogenic Sr and more radiogenic Nd and Pb) and 'Group II' to the 'micaceous' kimberlites (more radiogenic Sr and less radiogenic Nd and Pb). Mitchell and Bergman (1991) and Mitchell (1995) suggested that Group II kimberlites were renamed as 'orangeites' in recognition of their geographic abundance in the Orange Free State of South Africa, in addition to their distinct mineralogy and geochemistry. It was initially assumed that orangeites only occur within the Kaapvaal Craton, having formed seemingly uniquely during a limited time period in the Mesozoic (Skinner, 1989;

* Corresponding author. Tel. +91 9935647365 (Mobile).
E-mail address: nvcr100@gmail.com (N.V.C. Rao).
Peer-review under responsibility of China University of Geosciences (Beijing).

http://dx.doi.org/10.1016/j.gsf.2016.05.007

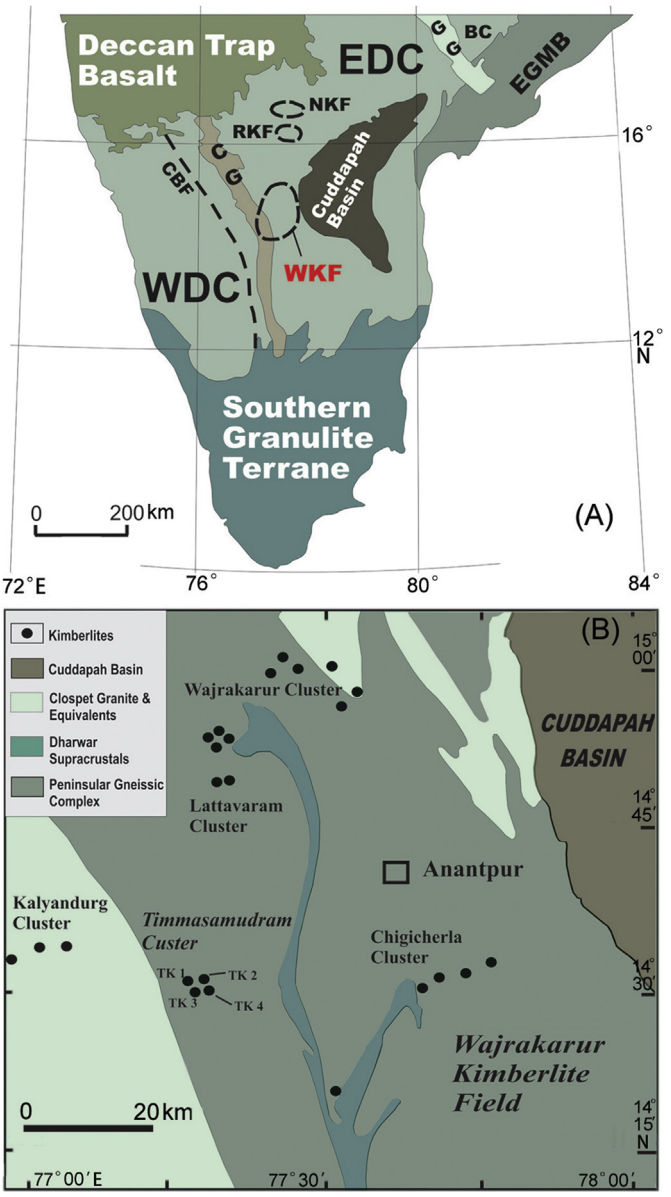

Figure 1. (A) Geological map of southern India showing location of Wajrakarur Kimberlite Field modified after Drury et al. (1984) and Patel et al. (2009). EDC: Eastern Dharwar Craton, WDC: Western Dharwar Craton, EGMB: Eastern Ghat Mobile Belt, CG: Closepet granite, NKF: Narayanpet kimberlite field, RKF: Raichur kimberlite field, WKF: Wajrakarur kimberlite field, CBF: Chitradurga boundary fault; (B) Enlarged map of Wajrakarur Kimberlite Field showing locations of Timmasamudram kimberlite cluster (TK-1 to TK-4 pipes) (after Nayak and Kudari, 1999).

Mitchell, 1995; Coe et al., 2008). However, subsequently rocks which are petrologically and geochemically akin to orangeite have been discovered in a number of other locations word-wide, e.g. Dronning Maud Land, Antarctica (ca. 159 Ma; Romu et al., 2008), the Mainpur area of the Bastar Craton, central India (ca. 65 Ma; Lehmann et al., 2010), and West Karelia (ca. 1.2 Ga; Kargin et al., 2014). A relatively rare, third group of kimberlitic intrusions termed as 'transitional' kimberlite were also recognized on the Kaapvaal Craton, as well as within the adjacent Proterozoic Namaqua–Natal mobile belt (Skinner et al., 1992; Becker et al., 2007). Subsequently, kimberlites with transitional petrological and geochemical characteristics were also described from various other cratons outside the southern African region (Beard et al., 2000; Kaminsky et al., 2004; Chalapathi Rao, 2005; Chalapathi Rao and Dongre, 2009).

All of the reported kimberlite occurrences in southern India are located on the Eastern Dharwar Craton (EDC), which represent one of the largest known Mesoproterozoic kimberlite provinces in the world (with an age of ~1100 Ma; Kumar et al., 2007a,b; Chalapathi Rao et al., 2013). More recently, the discovery of a late Cretaceous episode of kimberlite magmatism (~90 Ma) in the Timmasamudram cluster (TKC) of the EDC in southern India (Chalapathi Rao et al., 2016), has served to highlight the presence of at least two episodes of kimberlite magmatism on the EDC.

The Mesoproterozoic to late Cretaceous diamondiferous Timmasamudram kimberlite cluster is, thus, one of the very few clusters of the world, outside southern Africa, where kimberlites and orangeites occur together and serve to refine their petrogenetic and geodynamic models. The present study focuses on the mineralogical and petrological characteristics of the TKC (comprising of the TK-1, TK-2, TK-3 and TK-4 intrusions). One of the pipes in this cluster (the TK-1 macrocrystic variety) has recently been dated as late Cretaceous in age (~90 Ma), which contrasts with the ~1100 Ma Mesoproterozoic age of the TK-1 (microcystic variety) and the TK-3 intrusions (Chalapathi Rao et al., 2016). The purpose of the present contribution on the TKC, is (i) to document the mineral chemical compositions of groundmass phases in order to gain an understanding of magma liquidus compositions, (ii) to compare this new data with that available for other well characterised kimberlites and orangeites in India and southern Africa, in order to decipher similarities and differences, and (iii) to constrain their genesis from the new and previously published bulk-rock geochemical data, so as to gain insight into the geodynamics involved.

2. Geological setting

The Archean Dharwar Craton consists of a combination of granite–greenstone terranes, as well as gneissic basement of tonalite–trondhjemite–granodiorite (TTG) composition (the Peninsular Gneiss; Naqvi and Rogers, 1987). The Craton is bordered by the Proterozoic Eastern Ghats Mobile Belt (EGMB) in the east, by the Archean Bastar Craton in the northeast, and is covered by the Cretaceous–Paleogene lava flows of the Deccan Large Igneous Province in the northwest (Fig. 1). A conspicuous feature of the Dharwar Craton is the north–south trending, ~400 km long and 20–30 km wide cluster of plutons known as the Closepet Granite, dated at 2510 Ma (Friend and Nutman, 1991). Sediments of Paleo-Mesoproterozoic intra-cratonic sedimentary basins, such as the Cuddapah Basin, unconformably overlie the granite–greenstone terrane in the eastern region of the Dharwar Craton. The craton is divided into two blocks, the Eastern Dharwar Craton (EDC) and the Western Dharwar Craton (WDC), with apparently distinct histories of crustal evolution (Chadwick et al., 2000; Ramakrishnan and Vaidyanadhan, 2010). A prominent shear zone located along the eastern margin of the Chitradurga greenstone belt, the Chitradurga Boundary Fold (CBF), is widely considered to be the boundary between these blocks (Jayananda et al., 2006). Recent studies on kimberlite-derived eclogite xenoliths from the Wajrakarur kimberlite field (WKF), lend support to geodynamic models that favour the amalgamation of the Dharwar Craton through subduction (e.g. Dongre et al., 2015).

The kimberlites on the Dharwar Craton are restricted to the EDC, east of the Chitradurga shear zone, and are mainly distributed over three fields. These include the Wajrakarur kimberlite field (WKF) in the southern part of the EDC and the Narayanpet kimberlite field (NKF) in the northern part of the EDC, with the Raichur kimberlite field (RKF) located between these two (Fig. 1). Most of the WKF pipes are diamondiferous, with more than 30 individual pipes distributed over four distinct clusters, the Wajrakarur, Chigicherla, Kalyandurg and the Timmasamudram (Nayak and Kudari, 1999; Chowdary et al.,

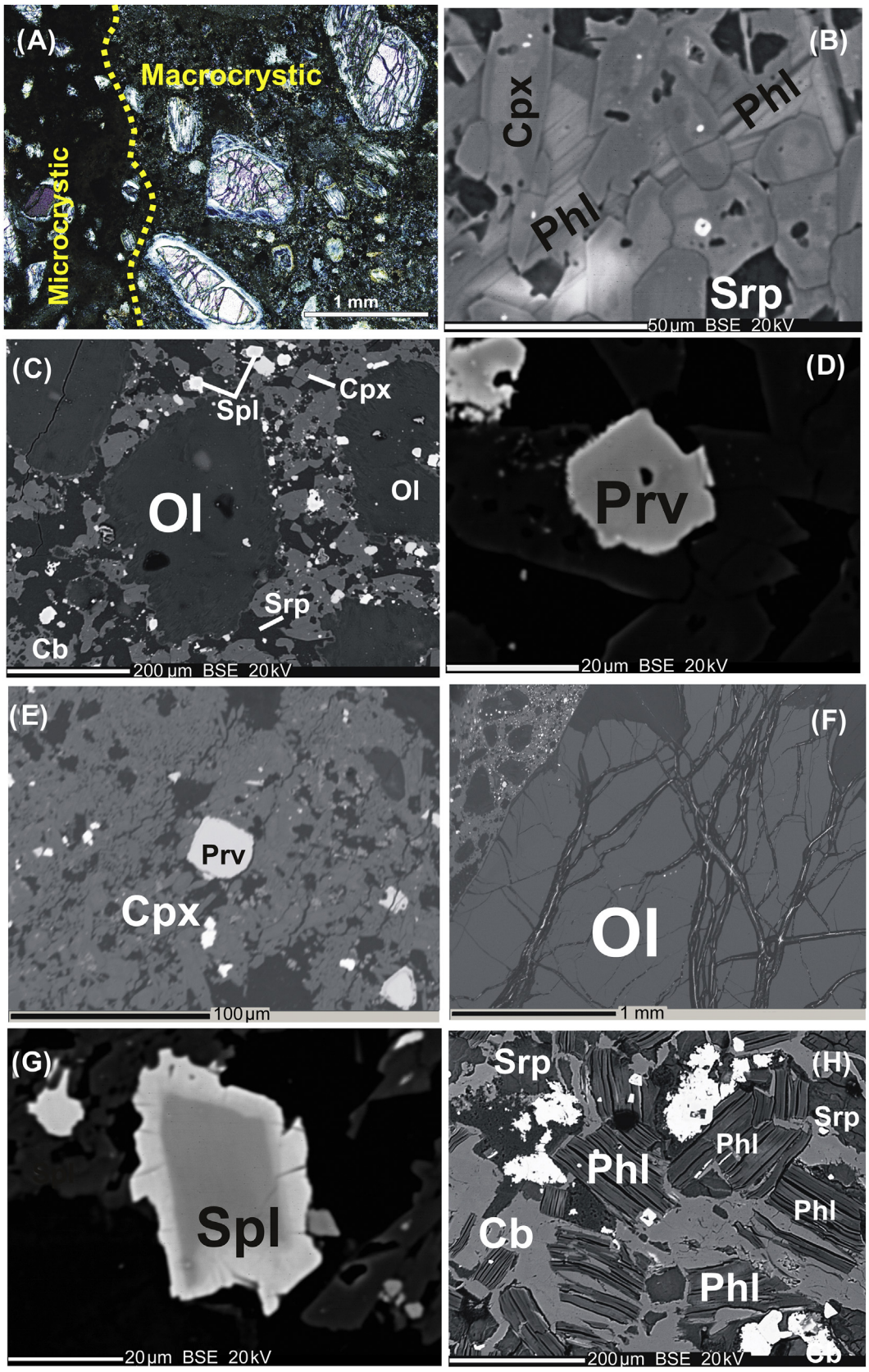

Figure 2. (A) Photomicrograph of TK-1 kimberlite in transmitted light showing a finer grained microcrystic variant having dark coloured groundmass (boundary demarcated by dotted line) and coarser grained macrocrystic variant; (B) BSE image of TK-1 (macrocrystic) showing association of phlogopite (Phl), clinopyroxene (Cpx) and serpentine (Srp) in the groundmass; (C) Inequigranular texture of TK-1 (macrocrystic) showing large olivine (Ol) in the groundmass rich in spinel (Spl), perovskite (Prv), carbonate (Cb), clinopyroxene and serpentine; (D) Unaltered perovskite in TK-1 (macrocrystic); (E) Clinopyroxene and perovskite association in the groundmass of TK-1 (macrocrystic) kimberlite; (F) Large olivine macrocryst in TK-1 kimberlite; (G) Zonned spinel in TK-1 (microcrystic) showing dark colour Cr rich core and irregular boundaries and (H) Groundmass texture of TK-4 (macrocrystic) kimberlite exceptionally rich in phlogopite, carbonate and serpentine.

2007). Precise Rb–Sr and U–Pb radiometric ages, determined on phlogopite and perovskite separates, demonstrate that kimberlite emplacement in the EDC took place during the Mesoproterozoic at ~1100 Ma (Gopalan and Kumar, 2008; Osborne et al., 2011; Chalapathi Rao et al., 2013), and again during the late Cretaceous at ~90 Ma (Chalapathi Rao et al., 2016).

The Timmasamudram kimberlite cluster (TKC) was discovered underneath diamondiferous river terrace gravels, by the Geological Survey of India during the 3-year period 2005–2007 (Chowdary et al., 2007). It is located on the left bank of the Penner River approximately 1.5 km WSW of the village of Timmasamudram. The surface expressions of these kimberlites are semi-circular to oval in shape, with pipe dimensions varying from 20 m × 25 m to 30 m × 50 m. The kimberlites are emplaced in TTG of the Peninsular Gneissic Complex (PGC), with an early- to mid-Archean age. Three of the kimberlite pipes (TK-1, TK-2 and TK-3), occur in linear alignment over a distance of 1 km, while the remaining kimberlite (TK-4) occurs in an adjacent, parallel fracture, approximately 0.6 km SE of TK-2 (Chowdary et al., 2007), and indicating a separate structural control for its emplacement. The processing of samples of the TKC by the Geological Survey of India, suggests that TK-1, TK-2 and TK-3 are barren. In contrast, a very high incidence of diamonds of gem quality, the highest recorded so far for any of the kimberlites in India, was encountered in TK-4 (Sridhar and Sinha, 2008).

3. Analytical procedure

The freshest possible samples were collected from outcrop, as well as exploration pits and trenches dug by the Geological Survey of India. Special care was taken to remove all visible crustal and mantle-derived contaminants, as well as calcite veining, before subjecting the samples to geochemical analysis. Mineral chemistry data were obtained on CAMECA SX-100 electron microprobes (EPMA) at TU Clausthal (Germany) as well as the University of Johannesburg (South Africa). Wavelength dispersive spectrometry (WDS), utilising TAP, LLIF and PET crystals, were employed. Various in-house standards were used for calibration, along with an acceleration voltage of 15 kV, a beam current of 20 nA, a beam diameter of 1 μm, and a counting time of 30 s. Whole-rock major and trace element analyses were conducted by Activation Laboratories Ltd., located in Ancaster, Ontario, Canada. ICP-OES (Thermo-JarretAsh ENVIRO II) was used to analyze the major elements, while ICP-MS (PerkinElmer Sciex ELAN 6000) was used to analyze the trace and rare earth elements (REE). The precision is <5% for all analyzed elements, at 100 × detection limit. Standards SY-3, W-2, DNC-1, BIR-1 and STM-1 were analysed along with the samples to check accuracy and precision. Further detail on the analytical procedure can be obtained from Gale et al. (1997) as well as the Activation Laboratories website (http://www.actlabs.com).

4. Petrography and mineral chemistry

All of the Timmasamudram kimberlites (i.e. TK-1, TK-2, TK-3 and TK-4) possess an inequigranular porphyritic texture, which is imparted by large rounded macrocrysts and microphenocrysts of olivine (sometimes serpentinised and carbonated) and phlogopite. TK-1 and TK-4 contain two distinct kimberlite varieties (Fig. 2A), comprising of comparatively fine-grained microcrystic kimberlite, as well as a coarser, macrocrystic variant (Sridhar and Sinha, 2008; Chalapathi Rao et al., 2016). These two variants are readily distinguishable in thin sections, and more rarely, also in hand specimen. In the case of the TK-1 kimberlite it has been demonstrated that the microcrystic kimberlite is older than the macrocrystic kimberlite (Chalapathi Rao et al., 2016). There are also sufficient major and trace element differences between the two TK-1 phases to suggest that they represent different batches of kimberlite magma (discussed further in geochemistry section of this paper). Relative age relations between the microcrystic and the macrocrystic kimberlite of the TK-4 pipe could not be determined (Sridhar and Sinha, 2008). The TK-1 kimberlite (macrocrystic) is the freshest among all the kimberlites of this cluster, and contain large macrocrysts of fresh, rounded to angular olivines, set in finer grained groundmass of olivine, phlogopite, clinopyroxene, spinel, calcite, ilmenite, apatite and perovskite (Fig. 2). Angular fragments (xenoliths) of the earlier formed microcrystic variant is comparatively finer-grained, but has a similar mineralogy to that of the macrocrystic variant, with the exception of the additional presence of phlogopite. Perovskite is more abundant in the microcrystic variant relative to the macrocrystic variant. In contrast, the macrocrystic variant of the TK-4 kimberlite pipe is extremely rich in phlogopite, which occurs both as macrocrysts and groundmass microphenocrysts (Fig. 2). Olivine macrocrysts are completely pseudomorphed by serpentine and carbonates. The groundmass is made up of olivine, phlogopite, spinel, calcite and perovskite. Shaikh et al. (2015) did not report the presence of perovskite in their study of the TK-4 kimberlite. Only macrocrystic, and not aphanitic, variants of TK-4 are incorporated in the present study, hence throughout this paper, TK-4 refers to the macrocrystic variant, unless otherwise specified. The rest of the kimberlites (TK-2 and TK-3) contain large rounded pseudomorphic macrocrysts and microphenocrysts of olivine and phlogopite, set in a fine grained, highly altered, serpentinised and carbonated groundmass rich in phlogopite, perovskite, ilmenite and spinel. All the TKC kimberlites contain crustal xenoliths of granitoid gneisses and amphibolites and ~1 to 3 cm-sized mantle nodules of phlogopite–garnet lherzolites and glimmerite (Chowdary et al., 2007; Sridhar and Sinha, 2008). However, no xenoliths were encountered during this study. The mineral chemistry of various primary phases in the TKC kimberlites (spinel, phlogopite, perovskite, olivine, clinopyroxene), is presented in Supplementary Tables 1–5, and compositional trends for each mineral are discussed below.

4.1. Spinel

Spinel grains (<50 μm) are present in all the samples examined, typically occurring as subhedral to euhedral crystals in the groundmass. Spinels in TK-1 (macrocrystic variety) show corroded and resorbed boundaries.

Two populations of spinel, which show little variation in terms of morphology, can be distinguished in TK-1, based on MgO and Cr_2O_3 contents (Supplementary Table 1): (i) chrome-spinels having higher MgO (up to 12.2 wt.%) and high Cr_2O_3 (6.6–49.2 wt.%, Cr/(Cr + Al): 0.70–0.96) occurring in the TK-1 macrocrystic variety of kimberlite and (ii) low Cr-spinels having lower MgO (up to 8.9 wt.%) and highly variable Cr_2O_3 (up to 0.07–48 wt.%, Cr/(Cr + Al): 0.08–0.96) in the TK-1 microcrystic variety. These populations likely reflect compositional differences between the two different kimberlite pulses in TK-1.

An abundance of chrome-spinel (Cr_2O_3 up to 59.2 wt.%, MgO up to 12.9 wt.% and Cr/(Cr + Al): 0.05–0.93) is a characteristic feature of TK-4. Two compositional trends are known for groundmass spinel from kimberlites, being (i) a magmatic trend-1, or the magnesian ulvospinel trend; and (ii) a magmatic trend-2, or the titano-magnetite trend (Mitchell, 1995). Kimberlite trend-1 is recognized as the characteristic, defining, spinel compositional trend of archetypal kimberlites (i.e. Group 1 kimberlites), whereas trend-2 is uncommon in Group 1 kimberlites but diagnostic of orangeites (i.e. Group 2 kimberlites) and ultramafic lamprophyres (Mitchell, 1995; Tappe et al., 2005). Interestingly, significant population of the spinels from all the pipes display the trend-2, also shown by spinels from the Bastar orangeites (Fig. 3). Many of the

spinels in TK-1 (microcrystic variety) are zoned, showing a decrease in Cr_2O_3 and MgO from core to margin. In contrast, the majority of the spinels in TK-1 (macrocrystic variety) are homogeneous.

4.2. Phlogopite

Phlogopite is abundant in the TK-1 (macrocrystic), TK-2, TK-3 and TK-4 kimberlites. In the TK-1 (macrocrystic variety) it mostly occurs as a groundmass phase, with occasionally-occurring spinel inclusions. Phlogopites in the TK-2 and TK-3 kimberlites are mostly chloritized. Those in the TK-4 pipe occur as irregular macrocrysts, as well as subhedral, distorted microphenocrysts. Mineral chemistry data and compositional trends for the phlogopites from TK-1 (macrocrystic) and TK-4 are presented in Supplementary Table 2 and Fig. 4. The phlogopites in TK-1 (macrocrystic) are depleted in Al_2O_3 (<10.2 wt.%) as well as in TiO_2 (<2.4 wt.%), and plot predominantly in the field of groundmass phlogopites in orangeites (Fig. 4A). Phlogopites in TK-4 are relatively enriched in TiO_2 (1.6–4.6 wt.%) and Al_2O_3 (11.6–15.3 wt.%) and follow the compositional trend of ultramafic lamprophyres (aillikites; Tappe et al., 2004), perhaps suggesting an affinity with such rocks for TK-4. However, higher Al_2O_3 content in phlogopite (than is typical for orangeites), have also been reported for phlogopites from the Bastar orangeites (Fig. 4A), while Ti-rich micas (TiO_2 up to 9 wt.%) have been also recognised in evolved orangeites at Besterskraal and Sover North (Mitchell, 1995). Phlogopites in the TK-1 (macrocrystic) and TK-4 kimberlites have higher FeO content than typical Group 1 kimberlites, are compositionally confined to the orangeite/lamproite field, and show some similarity to micas from the Bastar orangeites (Fig. 4B). Phlogopites in TK-1 (macrocrystic variety) follow the tetraferriphlogopite trend of increasing Fe accompanied by Al depletion, which is typical of orangeites (Mitchell, 1995). Cr_2O_3 contents vary widely with relatively higher contents in TK-4 (up to 1.2 wt.%), and lower contents (mostly <0.07 wt.%) in TK-1. The phlogopites in the various pipes under discussion show much variation in their K_2O and BaO contents, ranging from 5.3–10.1 wt.% and 0.2–4.4 wt.% respectively. The highest concentrations of Ba (up to 4.4 wt.%) are encountered in the groundmass micas of TK-1 (macrocrystic variety).

4.3. Perovskite

Perovskite is a common groundmass mineral in the TKC cluster, occurring as subhedral to euhedral grains. It is more abundant, and comparatively smaller in size (~10 μm), in the microcrystic variant of TK-1, as opposed to the macrocrystic variant. Perovskites show wide compositional variation in terms of their TiO_2 contents (TK-1 microcrystic variant: 51.1–57 wt.%; TK-1 macrocrystic variant: 49.4–58.7 wt.%; TK-3: 53.2–56 wt.%; TK-4: 46.2–62.4 wt.%; Supplementary Table 3) and REE_2O_3 (TK-1 microcrystic variant: 1.8–3.3 wt.%; TK-1 macrocrystic variant: 2–4.4 wt.%; TK-3: 4.1–6.4 wt.%; TK-4: 4.4–7.2 wt.%). Perovskites in TK-1 (macrocrystic), TK-3 and TK-4, with their higher TiO_2 and REE_2O_3 contents, display a marked compositional affinity with perovskites in orangeites (Donnelly et al., 2011, Fig. 5A).

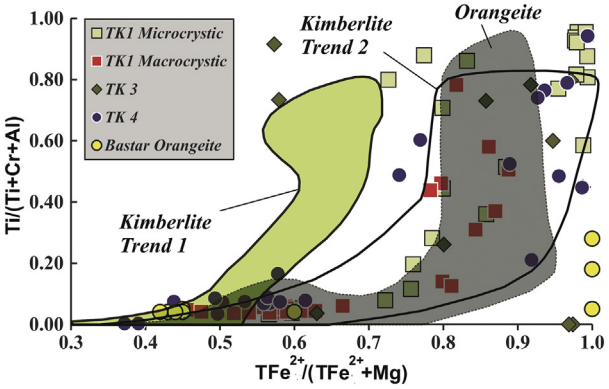

Figure 3. Atomic Ti/(Ti + Cr + Al) versus $TFe^{2+}/(TFe^{2+}+Mg)$ for spinels under study, fields after Mitchell (1995).

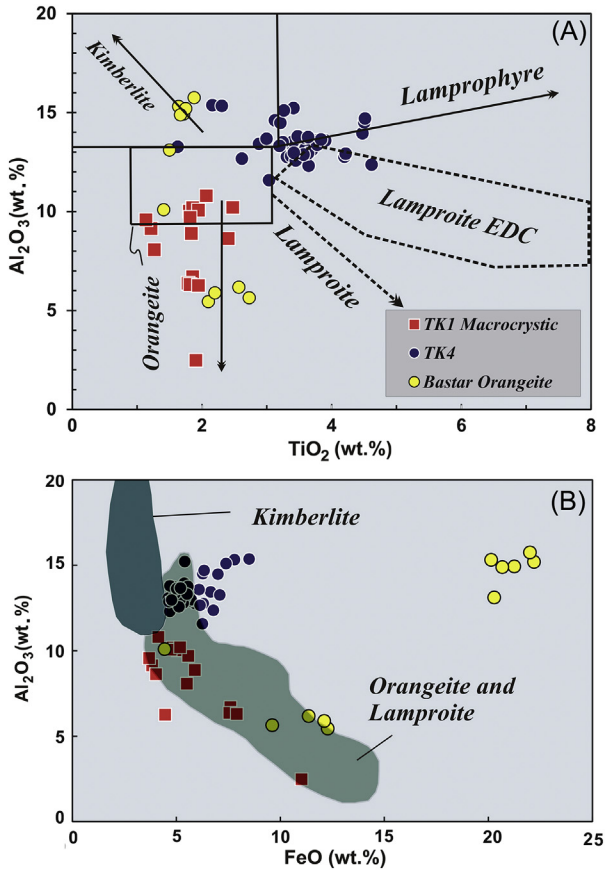

Figure 4. (A) TiO_2 versus Al_2O_3, and (B) FeO versus Al_2O_3 variation in phlogopite from TK-1 (macrocrystic variant) and TK-4 pipes. Fields for orangeite, kimberlite, lamproite and lamprophyres are from Mitchell (1995) and Beard et al. (2000); EDC lamproites from Chalapathi Rao et al. (2010); Bastar orangeites from Chalapathi Rao and Lehmann (2011).

4.4. Olivine

Macrocrystal and phenocrystal olivine are ubiquitous in the rocks of the TKC. Olivines in TK-1 are fresh, while those in TK-3 and TK-4 are mostly pseudomorphed by serpentine. The olivines in TK-1 (macrocrystic) are on average, more magnesian (Fo: 87.9–92.8; Fig. 4B) than in TK-1 (microcrystic), while those in TK-1 (microcrystic) are compositionally more diverse (Fo: 84.9–93.8; Supplementary Table 4 and Fig. 5B). This may be a reflection of source characteristics, e.g. olivines in orangeites tend to be slightly more magnesian than olivines in Group 1 kimberlites (Mitchell, 1995). Ni contents in both variants of the TK-1 pipe range from 0.29 to 0.42 wt.%.

4.5. Clinopyroxene

Clinopyroxene is present as small, unzoned, prismatic crystals in the groundmass of only TK-1 pipe. Shaikh et al. (2015) did report on

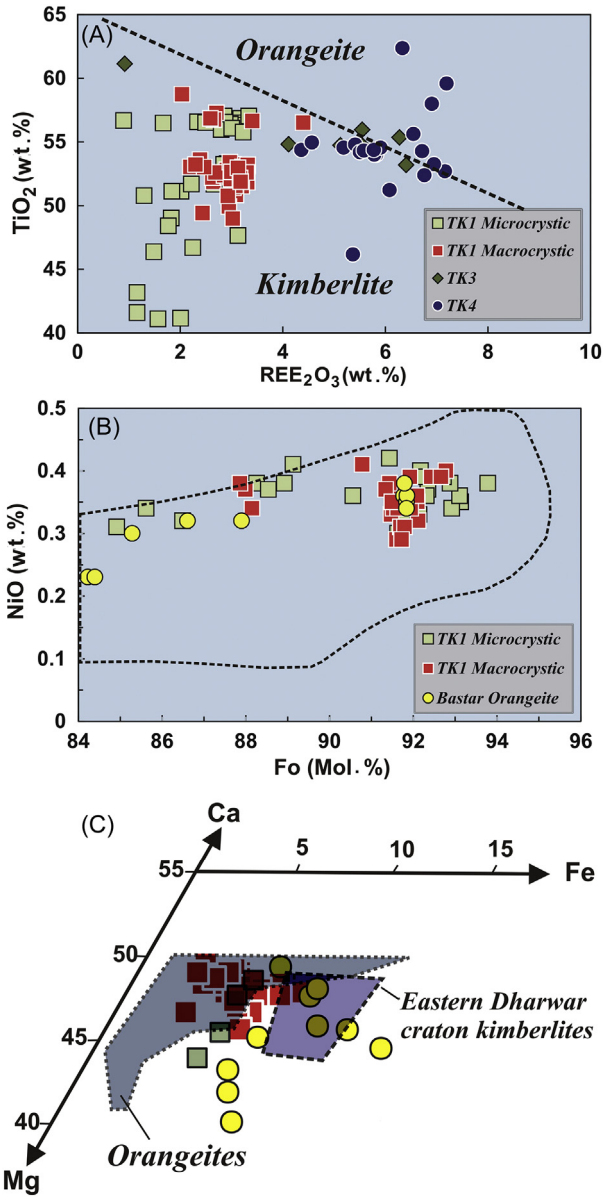

Figure 5. (A) TiO_2 versus ΣREE_2O_3 (La_2O_3, Ce_2O_3 and Nd_2O_3) variation for perovskites, dividing line between kimberlite and orangeites is from Donnelly et al. (2011); (B) NiO versus Fo variation for fresh olivines from TK1 pipe, kimberlite olivine field from Mitchell (1986); (C) Atomic Mg–Fe–Ca variation for clinopyroxenes from TK-1 kimberlite, fields for kimberlite and orangeite are from Mitchell (1995) and for Eastern Dharwar Craton kimberlites from Chalapathi Rao and Dongre (2009).

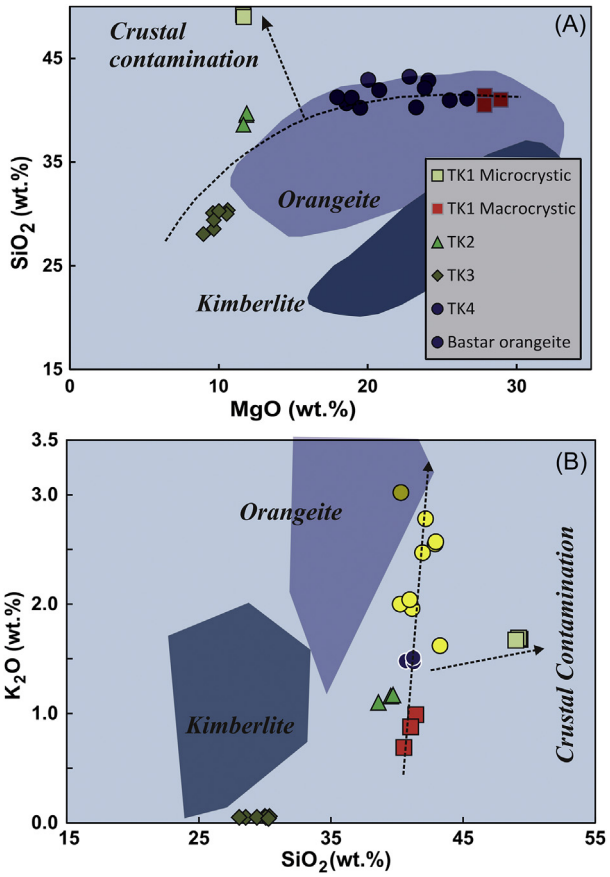

Figure 6. (A) MgO versus SiO_2, and (B) SiO_2 versus K_2O variation for kimberlites under study, fields for orangeite and kimberlite are from Becker and Le Roex (2006) and Becker et al. (2007).

the presence of clinopyroxene in TK-4, but chemical compositions were not determined. The clinopyroxene in the present study is a diopside of restricted compositional range, with little compositional difference between the macrocrystic and microcrystic variants (with the exception of Al_2O_3 and TiO_2). In the TK-1 microcrystic variant, Al_2O_3 varies up to 1.76 wt.% and TiO_2 up to 1.09 wt.%, while in the macrocrystic variant Al_2O_3 varies up to 0.88 wt.% and TiO_2 up to 3.27 wt.% (Supplementary Table 5). Primary groundmass clinopyroxene is generally a rare constituent in Group 1 kimberlites world-wide, with the exception of only a few occurrences (Zagodochnaya, Premier, Schuller, Orroroo; Mitchell, 1995 and references therein). In contrast, clinopyroxene is a common primary constituent of orangeites (Mitchell, 1995; Tappe et al., 2005; Coe et al., 2008), as well as the transitional kimberlites of southern Africa (Becker et al., 2007), and southern India (Chalapathi Rao and Dongre, 2009). The Fe–Mg–Ca compositions of clinopyroxenes at TK-1 (Fig. 5C) are comparable with Fe-poor diopsides occurring in orangeites from southern Africa (Mitchell, 1995) and central India (Chalapathi Rao et al., 2011), and are markedly different in composition to that of clinopyroxenes from EDC kimberlites which have much higher FeO contents (Fig. 5C).

5. Whole-rock geochemistry

New whole-rock major and trace element analyses of the TK-3 kimberlite are presented in Supplementary Table 6, along with existing available data for the TKC (Chalapathi Rao et al., 2016). The rocks are characterised by a wide variation in SiO_2 (28–49.3 wt.%), with TK-1 (microcrystic and macrocrystic varieties) and TK-4 (macrocrystic variety) showing the higher SiO_2 values (40.5–49.3 wt.%; Supplementary Table 6; Fig. 6A). These elevated SiO_2 contents are similar to that of (i.e. are characteristic of) orangeites from the Bastar Craton (Chalapathi Rao et al., 2011) as well as the Kaapvaal Craton (Becker and Le Roex, 2006). Marked geochemical differences are also observed for the microcrystic and macrocrystic variants of TK-1. The microcrystic variant contains lower MgO (~11 wt.%), higher CaO (~13 wt.%) and K_2O (~1.6 wt.%) whereas the macrocrystic variant is highly enriched in MgO (27–28 wt.%) and depleted in CaO (~7 wt.%) and K_2O (<1 wt.%) contents (Fig. 6B).

The diamondiferous TK-4 pipe shows higher bulk MgO (up to 18.91 wt.%) and $Mg^{\#}$ (83.80), similar to TK-1 (macrocrystic). MgO in samples from TK-2 and TK-3 is relatively low, ranging from 8.97 to

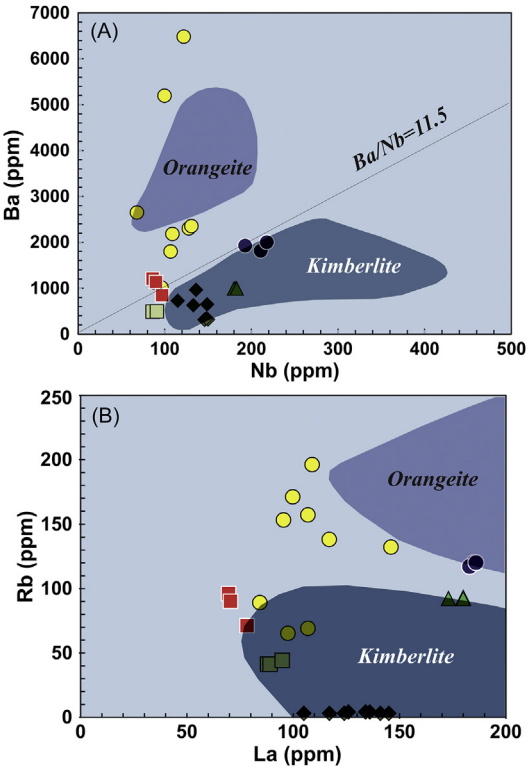

Figure 7. (A) Nb vs. Ba and (B) La vs. Rb variation for kimberlites under study, fields for kimberlites and orangeites are from Becker and Le Roex (2006).

11.88 wt.%, and is accompanied by a lower $Mg^{\#}$ (60–65). Lower $Mg^{\#}$ may result from water-rock interaction, and the leaching of MgO, as also reflected in the somewhat altered nature of these samples. $Fe_2O_3^T$ concentrations in all the pipes vary from 7 to 13.2 wt.%, whereas P_2O_5 contents are <1 wt.%. The TiO_2 content of bulk samples of the TKC pipes varies from 2–4 wt.%, with the exception of TK-1 (macrocrystic) and TK-4, which have the lowest TiO_2 (about ~1 wt.%; Supplementary Table 6). Such low TiO_2 is also a characteristic feature of the orangeites from the Bastar and Kaapvaal cratons. On plots of major element variation (Fig. 6), TK-1 (macrocrystic) and TK-4 samples are confined to the field of orangeites.

The samples of TK-1 (macrocrystic) and TK-4 have similar abundances of Ni (640–1130 ppm) to orangeite, in contrast to the other pipes of the TKC where Ni is considerably lower (<600 ppm; Supplementary Table 6). High field strength elements (HFSE) which are generally regarded to be immobile during hydrothermal alteration are comparatively more abundant in TK-4 (La: 193–218 ppm, Th: 28–29 ppm, Nb: 193–218 ppm) compared to the rest of the pipes (La: 69.6–180 ppm, Th: 9.9–23.7 ppm, Nb: 86–183 ppm; Supplementary Table 6). Large ion lithophile element contents e.g. Rb (3–120 ppm) and Ba (310–1999 ppm) are highly variable in all the samples, with those from TK-1 (macrocrystic variant) and TK-4 showing the highest content of Rb (71–120 ppm) and Ba (845–1999 ppm), similar to those displayed by orangeites (Fig. 7).

Primitive mantle-normalized trace element abundances for the samples of the TKC show two distinct types of patterns (Fig. 8). Both variants of TK-1 and TK-4 have abundance patterns similar to that of orangeite (Fig. 8A), e.g. a positive Pb anomaly and negative Rb, K, Sr and Ti anomalies. Samples from TK-2 and TK-3 show parallel patterns with pronounced negative Rb, Ba and K anomalies, and somewhat less pronounced negative spikes in the case of Ti, which differs from orangeites (Fig. 8B). Positive Pb anomalies are characteristic of Kaapvaal Craton orangeites (Becker and Le Roex, 2006) and Bastar orangeites (Chalapathi Rao et al., 2011), but are absent in the samples from TK-2 and TK-3.

6. Discussion

6.1. The effects of crustal contamination

Application of the crustal contamination index of Clement (1982) ($CI = (SiO_2 + Al_2O_3 + Na_2O)/(MgO + K_2O)$) to all the samples under investigation, results in a CI of 1.5–4.2 (Supplementary Table 6). Samples of TK-1 (microcrystic variety) show some of the highest CI values, even ranging up to 4.2. This implies a significant role for crustal contamination in this instance. In contrast, TK-1 (macrocrystic) shows some of the lowest CI values (~1.5), implying minimal crustal contamination. Moderately elevated CI values (~3) in the case of samples from TK-2 and TK-3 can be attributed to very low amounts of MgO and K_2O in these pipes, owing to the effects of secondary alteration as opposed to crustal contamination. Kjarsgaard et al. (2009) evaluated the applicability of the CI as a measure of contamination, and demonstrated the need to use it in conjunction with other geochemical screens. Therefore, in an attempt to further evaluate the degree of crustal contamination in the present instance, we have used binary diagrams which involve Si, Mg and fluid mobile elements such as K. On a plot of MgO versus SiO_2 (Fig. 6A), a general non-scattered positive trend is shown by all the samples with the exception of TK-1 (microcrystic). Elevated SiO_2 contents in the latter reflect the possible effects of crustal contamination. TK-1 (macrocrystic) and TK-4 samples shows elevated contents of K_2O similar to Indian and South African orangeites, reflecting higher modal amounts of phlogopite in these rocks. A general off-trend pattern for the samples of TK-1 (microcrystic variety) can also be seen on a plot of SiO_2 and K_2O (Fig. 6B), which once again, implies crustal contamination. However, a positive trend involving fluid mobile element K argues against crustal contamination in other samples. TK-4 and both variants of TK-1 also show positive Pb anomalies ($Pb/Pb^* = 1.7–3.9$) with TK-1 (microcrystic) having the highest values ($Pb/Pb^* = 3.4–3.9$; Fig. 9A). Crustal rocks are recognised as having higher Pb contents, and therefore such high positive Pb anomalies can be generated through crustal contamination. TK-1 (macrocrystic) and TK-4 also show similar lower abundances of HREE like those found in orangeites whereas TK-1 (microcrystic variant) shows higher HREE abundances (with Lu/Gd: 0.05; Fig. 9A). Importantly, higher HREE abundances and positive Pb anomalies are probably more likely due to crustal contamination (Le Roex et al., 2003), and hence probably not due to an orangeitic nature of the magma.

6.2. Orangeite nature of TK-1 (macrocrystic) and TK-4

The nomenclature of the primary host rock to the diamonds of the EDC remains controversial. Haggerty and Birkett (2004) commented on the absence of archetypal kimberlites, and classic lamproites, on the Indian Cratons. Paul et al. (2006, 2007) concluded that the Indian kimberlites show a transitional nature somewhere between southern African kimberlites, and lamproites of Western Australia. More recently, some of the kimberlites from the WKF have been re-classified as lamproites based solely on mineralogical grounds (Mitchell, 2010; Kaur and Mitchell, 2013, 2015). However, the present study clearly highlights the existence of kimberlite- and orangeite-type rocks in the TKC, through a combination of mineralogy and geochemistry.

The lower TiO_2, and the higher SiO_2 and K_2O content of TK-1 (macrocrystic) and TK-4 reflects their orangeitic nature (Smith et al., 1985; Becker and Le Roex, 2006). Bi-variate plots between

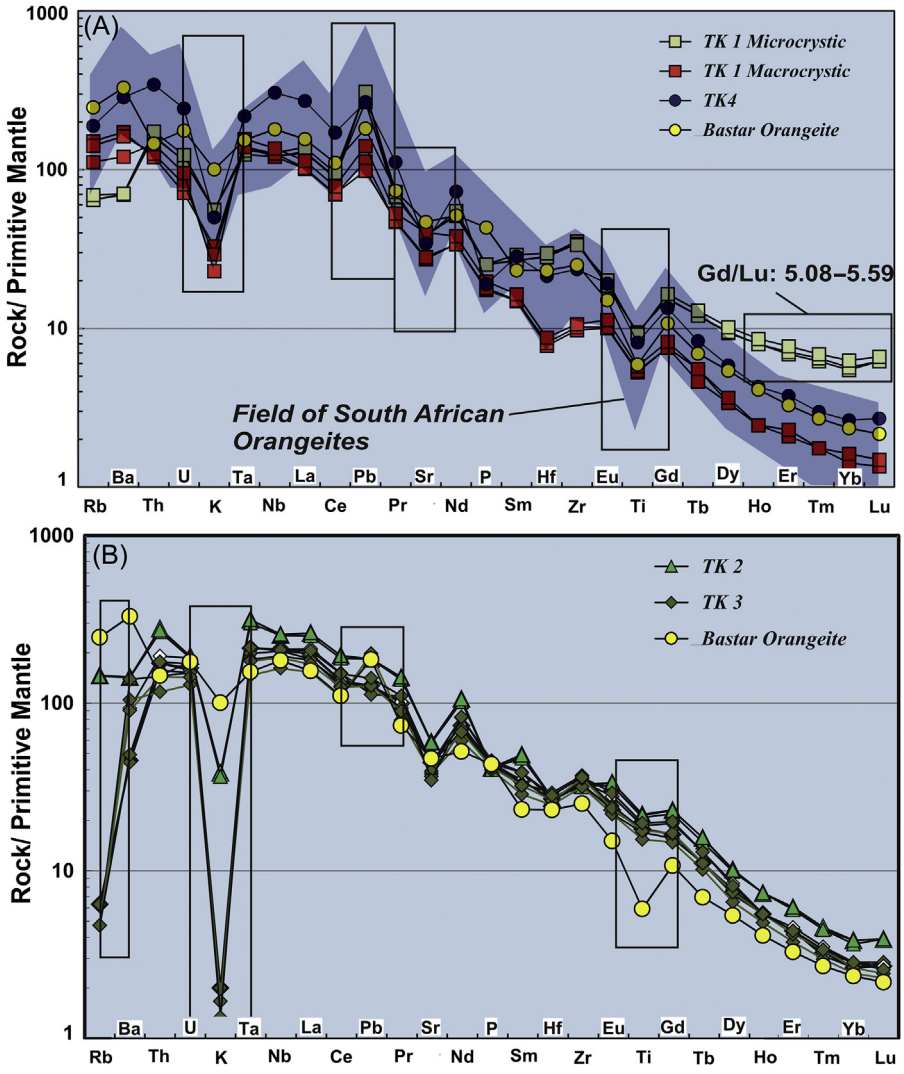

Figure 8. Primitive mantle normalized multi element plot for TK-1 and TK-4 kimberlites (A) and TK-2 and TK-3 kimberlites (B). Orangeite field from Becker and Le Roex (2006), normalizing values are from Sun and McDonough (1989).

LIL and HFS elements e.g. La–Rb and Nb–Ba, also highlights the same aspect (Fig. 7). As LILE are known to be more sensitive to secondary alteration, we further tested our argument by using trace element ratios which are generally unchanged during secondary processes and also during magmatic fractionation. Plots of Pb anomaly vs. Lu/Gd, Ba/Nb vs. Ce/Pb and La/Yb vs. La/Sm all show marked orangeitic affinity for TK-1 (macrocrystic) and TK-4 (Fig. 9 A–C). Furthermore, the mineral chemistry data also provides support to the orangeite classification of TK-1 (macrocrystic) and TK-4.

In situ perovskite dating yields a $^{206}Pb/^{238}U$ age of 1086 ± 19 Ma for TK-1 (microcrystic) and 1119 ± 12 Ma for TK-3, and a significantly younger late Cretaceous age of 86.8 ± 3.4 Ma for TK-1 (macrocrystic; Chalapathi Rao et al., 2016). No age could be obtained for TK-4 due to pervasive alteration of the perovskites. The $(^{143}Nd/^{144}Nd)_i$ values for the perovskites from TKC kimberlites range from 0.51183 to 0.51231, with ε_{Nd} values of −8.12 to +7.93 (Chalapathi Rao et al., 2016). The more enriched values of ε_{Nd} (−5.31 to −8.12) for TK-1 (macrocrystic) further attest to its orangeitic character (Fig. 10). It is evident from a binary plot of ε_{Nd} versus $(^{143}Nd/^{144}Nd)_i$ (Fig. 10) that perovskite from TK-4 yields ε_{Nd} values of +5.20 to +7.93, which exceeds the accepted upper limit of ε_{Nd} for Group I kimberlites world-wide. We propose that this anomalously high value could be an artifact arising from the assumption of a kimberlite emplacement age of 1100 Ma. Mineralogical and geochemical characteristics imply an orangeitic nature for TK-4 similar to that of TK-1 (macrocrystic). Hence, by assuming an emplacement age of say 90 Ma (i.e. that of the TK-1 macrocrystic variant), an enriched ε_{Nd} value of −10.67 to −12.63 are calculated for Tk-4. Such values fall within the orangeite field, and follow the same mantle–array displayed by the TK-1 (macrocrystic) and the Bastar orangeites. It is further evident from Fig. 10 that the data for TK-1 (macrocrystic) and TK-4 (after assigning an emplacement age of 90 Ma) are more similar (i.e. comparable) to orangeites, than to lamproites and 'transitional' kimberlites. In contrast, the data for TK-1 (microcrystic) and TK-3 are clearly confined to the world-wide data field for archetypal kimberlites (Group 1 kimberlites).

6.3. Implication of different magmatic pulses in TKC

Multiple pulses (episodes) of kimberlite magma are clearly present in the TKC. In the case of TK-4, macrocrystic as well as microcrystic phases are observed within a single intrusion (Chowdary et al., 2007). Conventional wisdom dictates that the microcrystic texture in kimberlite originates from flow

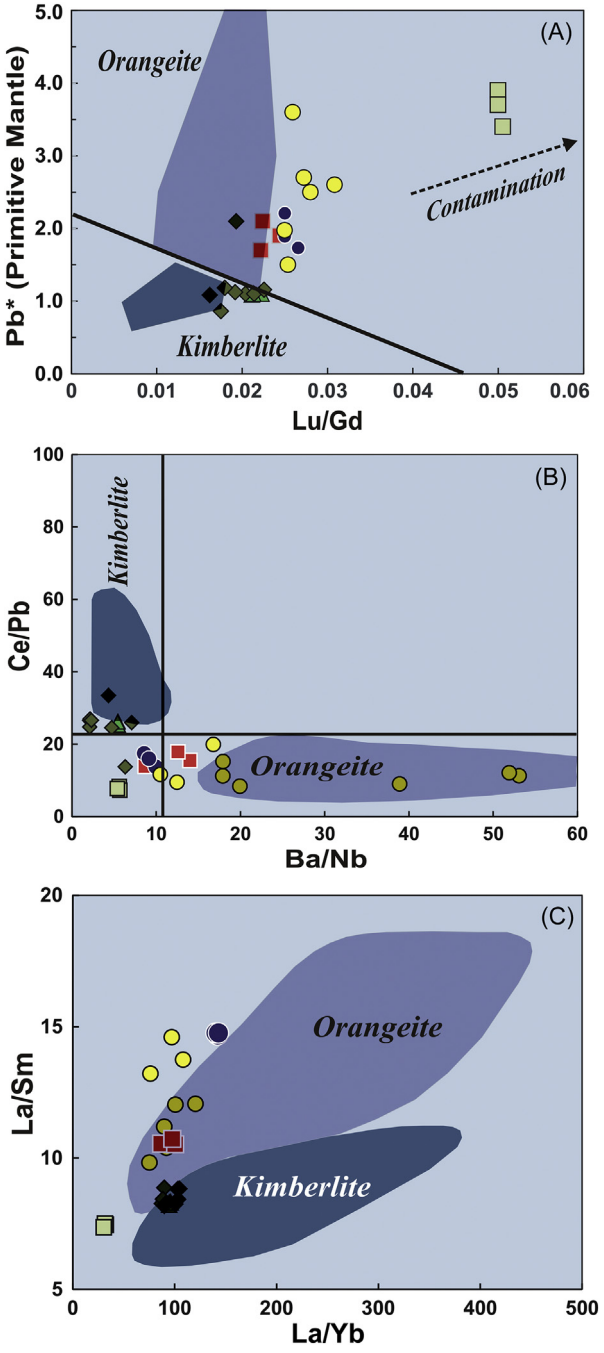

Figure 9. (A) Lu/Gd vs. Pb*, (B) Ba/Nb vs. Ce/Pb, and (C) La/Yb vs. La/Sm variations for kimberlites under study, data for orangeite and kimberlite fields from Becker and Le Roex (2006).

differentiation, where the larger macrocrysts are physically sorted and removed during ascent and emplacement (e.g. Bhattacharji, 1967; Komar, 1972; Mitchell, 1986; Shee, 1986; Scott Smith, 1996; Kjarsgaard, 2007), or crystal fractionation (Harris et al., 2004; Dongre et al., 2014), as opposed to multiple intrusions within the same pipe. Autoliths in kimberlites which are typically rounded and very fine grained (Dawson, 1980), compared to the host rock, and may represent samples of cognate magma (Patterson et al., 2008) and considered a result of magmatic liquation. In TK-1, two different variants (a microcrystic xenolithic variety, occurring in a macrocrystic host) are observed. These have sufficient mineralogical, major element, trace element, Nd isotope, and age differences,

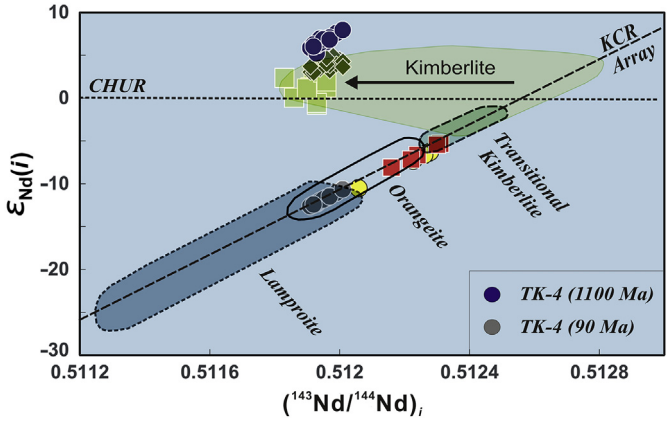

Figure 10. ε_{Nd} vs. $(^{143}Nd/^{144}Nd)_i$ plot for kimberlites under study (data from Chalapathi Rao et al., 2016). Fields of kimberlite, orangeite, lamproite and transitional kimberlites are compiled from the literature. Data sources: lamproite (Fraser et al., 1985; Davies et al., 2006), orangeite (Fraser et al., 1985; Nowell et al., 2004; Becker and Le Roex, 2006; Donnelly et al., 2011), kimberlite (Nowell et al., 2004; Becker and Le Roex, 2006; Carlson et al., 2006; Gaffney et al., 2007; Tappe et al., 2011; Tappe et al., 2013; Tappe et al., 2014) and transitional kimberlite (Nowell et al., 2004; Becker et al., 2007). Grey circles represent TK-4 kimberlite (after considering 90 Ma). Symbols for other kimberlites remain the same as in previous figures. KCR: kimberlite clan rocks.

to demonstrate that their derivation from different (separate) batches of kimberlite magma, and discount the possibility of being autoliths.

Kimberlites with more than one age population of perovskite, representing xenoliths of an earlier phase of kimberlite intrusion, occur in the Elliott County and Buffonta kimberlite clusters (Heaman and Kjarsgaard, 2000; Heaman et al., 2004). A spatial association of Paleoproterozoic Group I kimberlite and Cretaceous Group II kimberlite has been documented in the Kuruman province on the Kaapvaal Craton (Donnelly et al., 2011). Multiple phases of kimberlite magma, with distinct mineral modes, are also reported from the Pipe 2 kimberlite, WKF, India (Dongre et al., 2014), but their age relation remain unknown. A further isotopic and geochronological investigation of all the kimberlites of the WKF is required, in view of the presence of multiple emplacement ages of kimberlites on the EDC.

6.4. Magma generation

Pronounced negative Rb and K anomalies, as well as somewhat less pronounced Sr, P, Hf and Ti anomalies, are characteristics of Kaapvaal Craton kimberlites (i.e. Group 1-type kimberlites; Becker and Le Roex, 2006). Kaapvaal orangeites, in contrast, have (i) less prominent depletions of Rb and K, (ii) enriched patterns with relative depletions in Sr, P, Hf and Ti, (iii) a marked positive Pb anomaly, (iv) larger negative Ti anomalies and (v) broad depletion of K–Ta–Nb (Becker and Le Roex, 2006; Coe et al., 2008). Depletion in Nb and Ta is a characteristic feature of calc-alkaline magmatism, representing subduction-zone settings (e.g. Woodhead et al., 1998). Their presence in Kaapvaal orangeites is attributed to the metasomatism of their source regions by subduction-related upwelling of calc-alkaline fluids (Coe et al., 2008). It is important to note that subduction-related characteristics (Nb and Ta anomalies) are absent in orangeites from the TKC as well as the Bastar Craton (Fig. 8), and therefore is unlikely to have been derived from source regions that metasomatically-enriched by subduction-related fluids. However, their large negative Ti anomalies, together with their small

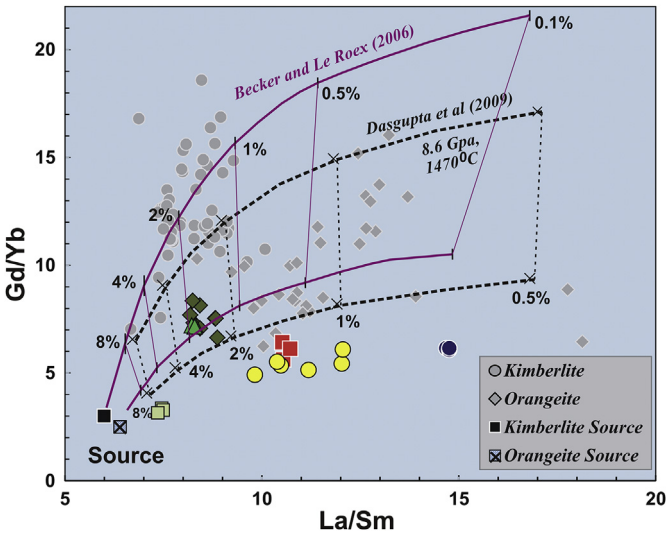

Figure 11. Gd/Yb vs. La/Sm for kimberlites under study. Illustrated curves represents melting trajectories of kimberlite and orangeites source regions. Source region compositions and residual modal mineralogy data is from Becker and Le Roex (2006). Numbers shown represents degree of melting. Melting curves in continuous line represents partition coefficients from Becker and Le Roex (2006), whereas melting curves in dashed line represents experimentally determined bulk peridotite/melt partition coefficients at 8.6 GPa and 1470 °C (from Dasgupta et al., 2009). Compositions of kimberlites (grey circles) and orangeites (grey diamonds) from South Africa are shown in background for comparison. Data for kimberlite and orangeite is from Le Roex et al. (2003), Becker and Le Roex (2006) and Coe et al. (2008). Symbols for TKC samples under study are same as in previous figures.

negative K and Rb anomalies, as well as their positive Pb anomalies, are characteristic features of orangeites world-wide.

Tappe et al. (2011, 2014) used experimentally determined peridotite/melt partition coefficients (Brey et al., 2008; Dasgupta et al., 2009) to calculate the trace element abundance patterns of partial melts forming between 6 and 10 GPa, utilizing a batch partial melting model. The incompatible trace element concentration levels of these calculated melts are mostly lower than actual concentrations observed in kimberlites. This difference in concentration can be addressed by lowering the assumed amount of partial melting, and/or using an enriched source composition. In Fig. 11 we have utilized the carbonated peridotite/melt partition coefficients given by Dasgupta et al. (2009), at 8.6 GPa and 1470 °C, for enriched source compositions inferred for South African kimberlites and orangeites on the Kaapvaal Craton (Becker and Le Roex, 2006). Experimental studies have shown that carbonatitic to kimberlitic melts can be generated by low degrees (F = 0.1–1%) of partial melting, of carbonated peridotite, at pressures between 5 and 10 GPa (Gudfinnsson and Presnall, 2005; Brey et al., 2008; Dasgupta et al., 2009; Foley et al., 2009). It can be deduced from Fig. 11 that the TKC and Bastar orangeites have relatively higher La/Sm that can be generated by low degrees of partial melting (F up to 1.5%). However, kimberlites have relatively lower La/Sm, requiring slightly higher amounts of partial melting (F > 1.5%). Contrasting La/Sm and Gd/Yb can be attributed to relatively more metasomatized (enriched) mantle source regions for orangeites (Becker and Le Roex, 2006). In another recent study, based on results from experimental melting of garnet peridotite at 6 GPa, the low Na_2O and FeO, but enriched K_2O, of orangeites are considered to have been derived from melt-depleted cratonic lithosphere, enriched by the metasomatic addition of K_2O- and H_2O-enriched fluids, and orangeite magmas can be constrained as being the product of ~0.2 wt.% melting of an enriched peridotite source (Novella and Frost, 2014). Recently, Giuliani et al. (2014) has also demonstrated the orangeite melt generation from an enriched mantle i.e. MARID-veined rich type of source.

6.5. Some geodynamic implications

The Nd isotopic compositions of perovskite from TK-1 (microcrystic) and TK-3 have a depleted signature, with T_{DM} Nd model ages of 1.2–1.3 Ga, and 1.4 Ga, respectively (Chalapathi Rao et al., 2016). This points to ancient metasomatic enrichment of their source regions during the Mesoproterozoic, similar to that of other EDC kimberlites that have been linked to the break-up of the Columbia supercontinent at 1300 Ma (Chalapathi Rao et al., 2013). The TK-1 (macrocrystic) and TK-4 sources, however, experienced relatively younger source enrichment with T_{DM} Nd model age of ~1100 Ma, which is similar to the source-enrichment age of the Bastar orangeites (Chalapathi Rao et al., 2011). This latter source-enrichment age, interestingly, coincides with the widespread emplacement of kimberlites and related rocks into the Eastern Dharwar and Bundelkhand Cratons of northern India, at 1100 Ma, which have been interpreted as representing the activity of a short-lived mantle plume during the Mesoproterozoic (Kumar et al., 2007a,b), as well as the timing of the assembly of the Rodinia supercontinent around 1000 Ma (Dalziel et al., 2000; Tappe et al., 2014).

The mantle-derived eclogite xenoliths from the KL-2 and P-3 kimberlite pipes of the WKF show evidence for a subduction-related origin, related to the amalgamation of the EDC (Dongre et al., 2015). However, due to the absence of radiometric ages for these xenoliths, the age of this geodynamic event remains unknown. In the case of South African orangeites, which shows depletion in Nb and other HFSE's, the involvement of subduction zone fluids for the enrichment of their lithospheric mantle source regions, has been invoked (Becker and Le Roex, 2006). Their Nd model ages coincide with a geodynamic event represented by the collision of the Proterozoic Namaqua–Natal belt and the Kaapvaal Craton at 1200 to 1000 Ma. The lack of characteristic negative Nb- and Ta-anomalies in the Indian orangeites excludes a subduction-related source enrichment process (Coe et al., 2008). Enrichment of mantle source regions has also been attributed to metasomatizing alkaline fluids or melts derived from upwelling asthenospheric mantle, which modify the overlying sub-continental lithospheric mantle (McKenzie, 1989; Foley, 1992; Le Roex et al., 2003; Tappe et al., 2012). Therefore, it is speculated that tectonic processes related to a 1100 Ma, short-lived plume activity, may have provided the heat resulting in (1) the initiation of partial melting, (2) the generation of the kimberlites on the EDC and the Bundelkhand Craton, (3) the depletion of the mantle source regions and (4) subsequently, or even contemporaneously, the enrichment of the already depleted source regions of the Indian orangeites. Thus, it appears that the amalgamation of the Rodinia supercontinent was associated with a short-lived mantle plume, which has played a key role in the eruption of 1100 Ma kimberlites, and the source enrichment of orangeites. However, recent work on the relation of kimberlites and supercontinent cycles, suggests a plate tectonic origin for kimberlites, without the melting of anomalously hot, upwelling mantle (Tappe et al., 2014). In general, the involvement of mantle plumes is held responsible for the disruption of supercontinents such as Columbia and Gondwana (Yoshida and Santosh, 2011). However, Chalapathi Rao et al. (2013) inferred that the 1100 Ma, short-lived plume activity, was inadequate in melting the shallow part of thick Indian lithosphere.

The enriched signature of TK-1 (macrocrystic) and highly diamondiferous TK-4 (assuming it was emplaced at 90 Ma)

necessitates their derivation from a long-lived, thick (>150 km) lithospheric mantle source. Heat-flow, magnetotelluric and seismic receiver function investigations indicate a much thinner modern day lithosphere thickness (<100 km) for the Eastern Dharwar Craton (Pandey and Agrawal, 1999; Gokarn et al., 2004; Kumar et al., 2007a,b). It has been argued that much of the lithospheric root beneath India may have been lost and/or modified during the breakup of Gondwana, and hence the (or during the) rapid northward drift of the Indian plate in the Cretaceous (Negi et al., 1986; Kumar et al., 2007a,b). However, the presence of diamondiferous orangeites of (i) ca. 65 Ma on the Bastar Craton, central India, and (ii) ca. 90 Ma on the Eastern Dharwar Craton, southern India, necessitates the survival of thick lithospheric roots up to at least the late Cretaceous (ca. 90 Ma) in the EDC, and up to 65 Ma in the case of the Bastar Craton (Lehmann et al., 2010; Chalapathi Rao and Lehmann, 2011), as the preservation of a rigid (cool) mantle keel extending into the diamond stability field is a requirement for the transport of diamonds to the earth's surface. If the geophysical perspective of a thinner modern-day Indian lithosphere is correct, then it is likely that interaction of the Indian plate with the Marion (at ca. 90 Ma) and the Reunion (at ca. 65 Ma) mantle plumes might have played a major role in the destruction of lithospheric roots by eroding the lower portions of the Indian plate, thereby facilitating its rapid northward movement after the late Cretaceous (Pandey and Agrawal, 1999; Veeraswamy and Raval, 2005; Kumar et al., 2007a,b; Eagles, 2013).

7. Conclusions

Mineral compositions of the various liquidus phases (spinel, phlogopite, clinopyroxene and perovskite) from all four kimberlites, and new whole-rock geochemical data for one of the pipes (TK-3), from the TKC, Wajrakarur field, Eastern Dharwar Craton, southern India, are presented. Amongst the TKC occurrences, the TK-1 (macrocrystic) and TK-4 intrusions show mineralogical signatures that are considered to be characteristic of orangeites viz., the presence of abundant macrocrysts and microphenocrysts of phlogopite, groundmass mica and titanomagnetite spinels displaying orangeite trends, higher REE_2O_3 contents in perovskites, and the presence of clinopyroxene of orangeitic affinity.

This mineralogical affinity towards orangeites is also supported by their geochemical characteristics such as higher SiO_2 and K_2O, lower TiO_2, higher Ba, Rb, Ba/Nb and La/Sm ratios, positive Pb anomalies, lower negative K anomalies, together with their enriched Nd isotopic (perovskite) signatures. On the other hand, the TK-1 microcrystic variety, as well as TK-2 and TK-3, have mineralogical and geochemical signatures more typical of archetypal kimberlites. Various geochemical screens involving major elements, Pb, and REE, provides evidence for the crustal contaminated nature of the TK-1 microcrystic variant.

Our forward batch melting modelling show the formation of orangeite and kimberlite melts by small degrees of partial melting of carbonated peridotite using carbonated peridotite/melt partition coefficients at 8.6 GPa with the orangeites requiring source regions that are more metasomatised than those of the kimberlites.

The absence of negative Nb, Ta and calc-alkaline signatures in the TKC orangeites exclude a Kaapvaal Craton – like subduction-related source enrichment in their generation. The recognition of the highly diamondiferous TK-4 and another TK-1 occurrence as an orangeite, with a possible emplacement age of ca. 90 Ma, has an important implication in that thick (>150 km) lithospheric mantle roots persisted in the southern Indian shield even after the breakup of the Gondwana supercontinent, till at least the late Cretaceous (ca. 90 Ma).

Acknowledgements

AD acknowledges financial support from the Department of Science and Technology, New Delhi, in the form of a major research project grant under the Fast Track Scheme for Young Scientists (No. SR/FTP/ES–175/2010). NVCR thanks the Head, Department of Geology, Banaras Hindu University, DST–SERB (lR/S4/ESF–18/2013), New Delhi and Alexander von Humboldt Foundation, Germany, for support. KSV acknowledges financial support from the South African Department of Science and Technology through their Research Chairs initiative (Geometallurgy), as administered by the National Research Foundation. The Centre of Excellence for Integrated Mineral and Energy Resource Analysis (CIMERA) at the University of Johannesburg is thanked for general funding, relating to this, and other projects. Felix Kaminsky made several useful comments on an earlier version of this manuscript. I.V. Aschepkov (Novosibirk) and another, unknown, reviewer are sincerely thanked for providing constructive reviews on this paper.

Appendix A. Supplementary data

Supplementary data related to this article can be found at http://dx.doi.org/10.1016/j.gsf.2016.05.007.

References

Beard, A.D., Downes, H., Hegner, E., Sablukov, S.M., 2000. Geochemistry and mineralogy of kimberlites from the Arkhangelsk Region, NW Russia: evidence for transitional kimberlite magma types. Lithos 51, 47–73.

Becker, M., Le Roex, A.P., 2006. Geochemistry of South African on- and off-craton Group I and II kimberlites: petrogenesis and source region evaluation. Journal of Petrology 47, 673–703.

Becker, M., Le Roex, A.P., Class, C., 2007. Geochemistry and petrogenesis of South African transitional kimberlites located on and off the Kaapvaal Craton. South African Journal of Geology 10, 631–646.

Bhattacharji, S., 1967. Mechanics of flow differentiation in ultramafic and mafic sills. Journal of Geology 75, 101–112.

Brey, G.P., Bulatov, V.K., Girnis, A.V., Lahaye, Y., 2008. Experimental melting of carbonated peridotite at 6–10 GPa. Journal of Petrology 49, 797–821.

Carlson, R.W., Czamanske, G., Fedorenko, V., Ilupin, I., 2006. A comparison of Siberian meimechites and kimberlites: implications for the source of high Mg alkalic magmas and flood basalts. Geochemistry, Geophysics, Geosystems 7, 1–21.

Chadwick, B., Vasudev, V.N., Hegde, G.V., 2000. The Dharwar Craton, southern India, interpreted as the result of Late Archaean oblique convergence. Precambrian Research 99, 91–111.

Chalapathi Rao, N.V., 2005. A petrological and geochemical reappraisal of the Mesoproterozoic diamondiferous Majhgawan pipe of central India: evidence for transitional kimberlite–orangeite (group II kimberlite)–lamproite rock type. Mineralogy and Petrology 84, 69–106.

Chalapathi Rao, N.V., Dongre, A.N., 2009. Mineralogy and geochemistry of kimberlites NK2 and KK6, Narayanpet kimberlite field, Eastern Dharwar craton, Southern India: evidence for a transitional kimberlite signature. Canadian Mineralogist 47, 1117–1135.

Chalapathi Rao, N.V., Lehmann, B., 2011. Kimberlites, flood basalts and mantle plumes: new insights from the Deccan large igneous province. Earth Science Reviews 107 (3), 315–324.

Chalapathi Rao, N.V., Kamde, G., Kale, H.S., Dongre, A.N., 2010. Petrogenesis of the Mesoproterozoic lamproites from the Krishna valley, eastern Dharwar Craton, southern India. Precambrian Research 177 (1), 103–130.

Chalapathi Rao, N.V., Lehmann, B., Mainkar, D., Belyatsky, B., 2011. Petrogenesis of the end-Cretaceous diamondiferous Behradih pipe: implication for mantle plume lithosphere interaction in the Bastar Craton, central India. Contributions to Mineralogy and Petrology 161, 721–742.

Chalapathi Rao, N.V., Wu, F.Y., Mitchell, R.H., Li, L.Q., Lehmann, B., 2013. Mesoproterozoic U–Pb ages, trace element and Sr–Nd isotopic composition of perovskite from kimberlites of the Eastern Dharwar craton, southern India: distinct mantle sources and a widespread 1.1 Ga tectonomagmatic event. Chemical Geology 353, 48–64.

Chalapathi Rao, N.V., Dongre, A.N., Wu, F.Y., Lehmann, B., 2016. A Late Cretaceous (ca. 90 Ma) kimberlite event in southern India: implication for sub-continental lithospheric mantle evolution and diamond exploration. Gondwana Research. http://dx.doi.org/10.1016/j.gr.2015.06.006.

Chowdary, V., Rau, T.K., Bhaskara Rao, K.S., Sridhar, M., Sinha, K.K., 2007. Timmasamudram kimberlite cluster, Wajrakarur kimberlite field, Anantapur district, Andhra Pradesh. Journal of the Geological Society of India 69, 567–610.

Clement, C.R., 1982. A Comparative Geological Study of Some Major Kimberlite Pipes in the Northern Cape and Orange Free State. Ph.D. Thesis. University of Cape Town.
Coe, N., Le Roex, A., Gurney, J.J., Pearson, G.D., Nowell, G., 2008. Petrogenesis of Swartruggens and Star Group II kimberlite dyke swarms, South Africa: constraints from whole rock geochemistry. Contributions to Mineralogy and Petrology 156, 627–652.
Dalziel, I.W.D., Mosher, S., Gahagan, L.M., 2000. Laurentia–Kalahari collision and the assembly of Rodinia. Journal of Geology 108, 499–513.
Dasgupta, R., Hirschman, M.M., McDonough, W.F., Spiegelman, M., Withers, A.C., 2009. Trace element partitioning between garnet lherzolite and carbonatite at 6.6 and 8.6 GPa with applications to the geochemistry of the mantle and of mantle-derived melts. Chemical Geology 262, 57–77.
Davies, G.R., Stolz, A.Z., Mahotkin, I.L., Nowell, G.M., Pearson, D.G., 2006. Trace element and Sr–Pb–Nd–Hf evidence for ancient, fluid dominated enrichment of the source of Aldan shield lamproites. Journal of Petrology 47, 1119–1146.
Dawson, J.B., 1980. Kimberlites and Their Xenoliths. Springer-Verlag, Berlin, Germany, p. 252.
Dongre, A., Chalapathi Rao, N.V., Malandkar, M., 2014. Petrogenesis of macrocrystic and aphanitic intrusions in Mesoproterozoic diamondiferous pipe 2 kimberlite, Wajrakarur kimberlite field, eastern Dharwar craton, southern India. Geochemical Journal 48 (5), 491–507.
Dongre, A.N., Jacob, D.E., Stern, R.A., 2015. Subduction-related origin of eclogite xenoliths from the Wajrakarur kimberlite field, Eastern Dharwar craton, Southern India: constraints from petrology and geochemistry. Geochimica et Cosmochimica Acta 166, 165–188.
Donnelly, C.L., Griffin, W.L., O'Reilly, S.Y., Pearson, N.J., Shee, S.R., 2011. The kimberlites and related rocks of the Kuruman kimberlite Province, Kaapvaal craton, South Africa. Contributions to Mineralogy and Petrology 161, 351–371.
Drury, S.A., Harris, N.B.W., Holt, R.W., Reeves-Smith, G.J., Wightman, R.T., 1984. Precambrian tectonics and crustal evolution in south India. Journal of Geology 92, 3–20.
Eagles, G., 2013. Ridge push, mantle plumes and the speed of Indian plate. Geophysical Journal International 194 (2), 670–677.
Foley, S.F., 1992. Vein-plus-wall-rock melting mechanisms in the lithosphere and the origin of potassic alkaline magmas. Lithos 28, 435–438.
Foley, S.F., Yaxley, G.M., Rosenthal, A., Buhre, S., Kiseeva, E.S., Rapp, R.P., Jacob, D.E., 2009. The composition of near-solidus melts of peridotite in the presence of CO_2 and H_2O between 40 and 60 kbar. Lithos 112, 274–283.
Fraser, K.J., Hawkesworth, C.J., Erlank, A.J., Mitchell, R.H., Scott-Smith, B.J., 1985. Sr, Nd, and Pb isotope and minor element geochemistry of lamproites and kimberlites. Earth and Planetary Science Letters 76, 57–70.
Friend, C.R.L., Nutman, A.P., 1991. SHRIMP U–Pb geochronology of the Closepet granite and peninsular gneisses, Karnataka, South of India. Journal Geological Society of India 38, 357–368.
Gaffney, A.M., Blichert-Toft, J., Nelson, B.K., Bizzarro, M., Rosing, M., Albarede, F., 2007. Constraints on source-forming processes of West Greenland kimberlites inferred from Hf–Nd isotope systematics. Geochimica et Cosmochimica Acta 71, 2820–2836.
Gale, G.H., Dabek, L.B., Fedikow, M.A.F., 1997. The application of rare earth element analyses in the exploration for volcanogenic massive sulfide type deposits. Exploration and Mining Geology 6, 233–252.
Gokarn, S.G., Gupta, G., Rao, C.K., 2004. Geoelectric structure of the Dharwar Craton from magnetotelluric studies: archean suture identified along the Chitradurga–Gadag schist belt. Geophysics Journal International 158, 712–758.
Gopalan, K., Kumar, Anil, 2008. Phlogopite K–Ca dating of Narayanpet kimberlites, South India: implications to the discordance between their Rb–Sr, Ar/Ar ages. Precambrian Research 67, 377–382.
Gudfinnsson, G.H., Presnall, D.C., 2005. Continuous gradations among primary carbonatitic,kimberlitic, melilititic, basaltic, picritic, and komatiitic melts in equilibrium with garnetlherzolite at 3–8 GPa. Journal of Petrology 46, 1645–1659.
Haggerty, S.E., Birkett, T., 2004. Geological setting and chemistry of kimberlite clan rocks in the Dharwar Craton, India. Lithos 76, 535–549.
Harris, M., Le Roex, A.P., Class, C., 2004. Geochemistry of the Uintiesberg kimberlite, South Africa: petrogenesis of an offcraton, group I kimberlite. Lithos 74, 149–165.
Heaman, L.M., Kjarsgaard, B.A., 2000. Timing of eastern North American kimberlite magmatism: continental extension of the Great Meteor hotspot track? Earth and Planetary Science Letters 178, 253–268.
Heaman, L.M., Kjarsgaard, B.A., Creaser, R.A., 2004. The temporal evolution of North American kimberlites. Lithos 76, 377–397.
Jayananda, M., Chardon, D., Peucat, J.J., Capdevila, R., 2006. 2.61 Ga potassic granites and crustal reworking in the western Dharwar craton, southern India: tectonic, geochronologic and tectonic constraints. Precambrian Research 150, 1–26.
Kaminsky, F.E., Sablukov, S.M., Sablukova, L.I., Chaner, D.M.D., 2004. Neoproterozoic 'anomalous' kimberlites of Guaniamo, Venezuela: mica kimberlites of 'isotopic transitional' type. Lithos 76, 565–590.
Kargin, A.V., Nosova, A.A., Larionova, Y.O., Kononova, V.A., Borisovsky, S.E., Koval'chuk, E.V., Griboedova, I.G., 2014. Mesoproterozoic orangeites (kimberlite II) of west Karelia: mineralogy, geochemistry and Sr–Nd isotope composition. Petrology 22, 151–183.
Kaur, G., Mitchell, R.H., 2013. Mineralogy of P2 west kimberlite, Wajrakarur kimberlite field, Andhra Pradesh, India: Kimberlite or lamproite? Mineralogical Magazine 77, 3175–3196.
Kaur, G., Mitchell, R.H., 2015. Mineralogy of P-12 K–Ti richterite–diopside–olivine lamproite from Wajrakarur, Andhra Pradesh, India: implications for subduction related magmatism in eastern India. Mineralogy and Petrology 110, 1–23.
Kjarsgaard, B.A., 2007. Kimberlite pipe models: significance for exploration. In: Milkereit, B. (Ed.), Proceedings of Exploration: Fifth Decennial International Conference on Mineral Exploration, pp. 667–677.
Kjarsgaard, B.A., Pearson, D.G., Tappe, S., Nowell, G.M., Dowall, D.P., 2009. Geochemistry of hypabyssal kimberlites from Lac de Gras, Canada: comparisons to a global database and applications to the parent magma problem. Lithos 112S, 236–248.
Komar, P.D., 1972. Flow differentiation in igneous dykes and sills; profiles of velocity and phenocryst concentration. Geological Society of America Bulletin 83, 3443–3447.
Kumar, Anil, Heaman, L.A., Manikyamba, C., 2007a. Mesoproterozoic kimberlites in south India: a possible link to ~1.1 Ga global magmatism. Precambrian Research 15, 192–204.
Kumar, P., Yuan, X., Kumar, R., Kind, R., Xuequing, L., Chadha, R.K., 2007b. The rapid drift of the Indian tectonic plate. Nature 449, 894–897.
Le Roex, A.P., Bell, D.R., Davis, P., 2003. Petrogenesis of Group I kimberlites from Kimberley, South Africa: evidence from bulk rock geochemistry. Journal of Petrology 44, 2261–2286.
Lehmann, B., Burgess, R., Frei, D., Belyatsky, B., Mainkar, D., Chalapathi Rao, N.V., Heaman, L.M., 2010. Diamondiferous kimberlites in Central India synchronous with the Deccan flood basalts. Earth and Planetary Science Letters 290, 142–149.
McKenzie, D., 1989. Some remarks on the movement of small melt fractions in the mantle. Earth and Planetary Science Letters 95, 53–72.
Mitchell, R.H., 1986. Kimberlites: Mineralogy, Geochemistry, and Petrology. Plenum, New York.
Mitchell, R.H., 1995. Kimberlites, Orangeites and Related Rocks. Plenum Press, New York, p. 410.
Mitchell, R.H., 2010. Mineralogy of the P2 West Kimberlite, Wajrakarur, AP, India 6th International Dyke Conference. Varanasi, India, 91. (abstract).
Mitchell, R.H., Bergman, S.C., 1991. Petrology of Lamproites. Plenum Press, New York, p. 408.
Naqvi, S.M., Rogers, J.J.W., 1987. Precambrian Geology of India. Oxford University Press, New York, p. 223.
Nayak, S.S., Kudari, S.A.D., 1999. Discovery of diamond-bearing kimberlites in Kalyandurg area, Anantapur district, Andhra Pradesh. Current Science 76, 1077–1079.
Negi, J.G., Pandey, O.P., Agrawal, P.K., 1986. Super mobility of hot Indian lithosphere. Tectonophysics 131, 147–156.
Novella, D., Frost, D.J., 2014. The composition of hydrous partial melts of Garnet peridotite at 6 Gpa: Implications for the origin of Group II kimberlites. Journal of Petrology 55, 2097–2124.
Nowell, G.M., Pearson, D.G., Bell, D.R., Carlson, R.W., Smith, C.B., Kempton, P.D.M., Noble, S.R., 2004. Hf isotope systematics of kimberlites and their megacrysts: new constraints on their source regions. Journal of Petrology 45, 1583–1612.
Osborne, I., Sherlock, S., Anand, S., Argles, T., Osborne, I., Sherlock, S., 2011. New Ar-Ar ages of southern Indian kimberlites and a lamproite and their geochemical evolution. Precambrian Research 189, 91–103.
Pandey, O.P., Agrawal, P.K., 1999. Lithospheric mantle deformation beneath the Indian cratons. Journal of Geology 107, 683–692.
Patel, S.C., Ravi, S., Kumar, Y.A., Naik, A., Thakur, S.S., Pati, J.K., 2009. Mafic xenoliths in Proterozoic kimberlites from Eastern Dharwar Craton, India:Mineralogy and P–T regime. Journal of Asian Earth Sciences 34, 336–346.
Patterson, M., Francis, D., McCandless, D., 2008. Autoliths as Samples of Kimberlite Magma. Goldschmidt Conference Abstract, A727.
Paul, D.K., Nayak, S.S., Pant, N.C., 2006. Indian kimberlites and related rocks: petrology and geochemistry. Journal Geological Society of India 67, 328–355.
Paul, D.K., Crocket, J.H., Reddy, T.A.K., Pant, N.C., 2007. Petrology and geochemistry including platinum group element abundances of the Mesoproterozoic ultramafic (lamproite) rocks of Krishna district, southern India: implications for source rock characteristics and petrogenesis. Journal of Geological Society of India 69, 577–596.
Ramakrishnan, M., Vaidyanadhan, R., 2010. Geology of India, 1. Geological Society of India, Bangalore.
Romu, I., Luttinen, A., O'Brien, H., 2008. Lamproite-orangeite Transition in 159 Ma Dykes of Dronning Maud Land, Antarctica?' (Abst.), 9th International Kimberlite Conference, 9IKC-A- 00362.
Scott Smith, B.H., 1996. Kimberlites. In: Mitchell, R.H. (Ed.), Undersaturated Alkaline Rocks: Mineralogy, Petrogenesis, and Economic Po-tential. Mineralogical Society of Canada, Short Course Series 24, pp. 217–243.
Shaikh, A.M., Patel, S.C., Ravi, S., 2015. Compositional Evolution of Phlogopites in TK-4 Kimberlite, Southern India. Goldschmidt abstracts 2854.
Shee, S.R., 1986. The Petrogenesis of the Wesselton Mine Kimberlites, Kimberley, South Africa. Ph.D. Thesis. University of Cape Town.
Skinner, E.M.W., 1989. Contrasting Group I and II kimberlite petrology: towards a genetic model for kimberlites. Geological Society of Australia. Special Publication 14 (1), 528–544.
Skinner, E.M.W., Smith, C.B., Viljoen, K.S., Clark, T.C., 1992. The petrography, tectonic setting and emplacement ages of kimberlites in the south western border region of the Kaapvaal Craton, Prieska area, South Africa. In: Meyer, H.O.A., Leonardos, O.H. (Eds.), Kimberlites, Related Rocks and Mantle Xenoliths. CPRM, Brasilia, pp. 80–97.

Smith, C.B., 1983. Pb, Sr and Nd isotopic evidences for sources of southern African Cretaceous kimberlites. Nature 304, 51–54.
Smith, C.B., Allsopp, H.L., Kramers, J.D., Hutchinson, G., Roddick, J.C., 1985. Emplacement ages of Jurassic-Cretaceous South African kimberlites by the Rb-Sr method on phlogopite and whole-rock samples. Transactions of the Geological Society of South Africa 88, 249–266.
Sridhar, M., Sinha, K.K., 2008. Testing of the diamondiferous nature of the newly discovered kimberlites in the Wajrakarur field, Anantapur district, Andhra Pradesh. Records of the Geological Survey of India 140 (Part-5), 25.
Sun, S.S., McDonough, W.F., 1989. Chemical and isotopic systematics of oceanic basalts: implications for mantle composition and processes. In: Saunders, A.D., Norry, M.J. (Eds.), Magmatism in Ocean Basins, 42. Geological Society of London Special Publication, pp. 313–345.
Tappe, S., Jenner, G.A., Foley, S.F., Heaman, L.M., Besserer, D., Kjarsgaard, B.A., Ryan, A.B., 2004. Torngat ultramafic lamprophyres and their relation to the North Atlantic Alkaline Province. Lithos 76, 491–518.
Tappe, S., Foley, S.F., Jenner, G.A., Kjarsgaard, B.A., 2005. Integrating ultramafic lamprophyres into the IUGS classification of igneous rocks: rational and implications. Journal of Petrology 46, 1893–1900.
Tappe, S., Pearson, D.G., Nowell, G., Nielsen, T., Milstead, P., Muehlenbachs, K., 2011. A fresh isotopic look at Greenland kimberlites: cratonic mantle lithosphere imprint on deep source signal. Earth and Planetary Science Letters 305, 235–248.
Tappe, S., Steenfelt, A., Nielsen, T.F.N., 2012. Asthenospheric source of Neoproterozoic and Mesozoic kimberlites from the North Atlantic craton, West Greenland: new high-precision U–Pb and Sr–Nd isotope data on perovskite. Chemical Geology 320, 113–127.
Tappe, S., Pearson, D.G., Kjarsgaard, B.A., Nowell, G.M., Dowall, D., 2013. Mantle transition zone input to kimberlite magmatism near a subduction zone: origin of anomalous Nd-Hf isotope systematics at Lac de Gras, Canada. Earth and Planetary Science Letters 371–372, 235–251.
Tappe, S., Kjarsgaard, B.A., Kurszlaukis, S., Nowell, G.M., Philips, D., 2014. Petrology and Nd–Hf isotope geochemistry of the Neoproterozoic Amon kimberlite sills, Baffin Island (Canada): evidence for deep mantle magmatic activity linked to supercontinent cycles. Journal of Petrology 55, 2003–2042.
Veeraswamy, K., Raval, U., 2005. Remobilization of the paleoconvergent corridors hidden under the Deccan Trap cover and some major stable continental region earthquakes. Current Science 89 (3), 522–530.
Wagner, P.A., 1914. The Diamond Fields of South Africa. Transvaal Leader, Johannesburg, South Africa.
Woodhead, J.D., Eggins, S.M., Johnson, R.W., 1998. Magma genesis in the New Britain Island Arc: further insights into melting and mass transfer process. Journal of Petrology 39, 1641–1668.
Yoshida, M., Santosh, M., 2011. Supercontinents, mantle dynamics and plate tectonics: a perspective based on conceptual vs numerical models. Earth Science Reviews 105, 1–24.